Received: 1 May 2020 | Revised: 14 December 2020 | Accepted: 7 June 2021

DOI: 10.1111/jfr3.12738

ORIGINAL ARTICLE

CIWEM Chartered Institution of Water and Environmental Management | Journal of Flood Risk Management | WILEY

Assessing the risk of vehicle instability due to flooding

Ricardo A. Bocanegra | **Félix Francés**

Research Institute of Water and Environmental Engineering (IIAMA), Universitat Politècnica de València, Valencia, Spain

Correspondence
Ricardo A. Bocanegra, Research Institute of Water and Environmental Engineering (IIAMA), Universitat Politècnica de València, Valencia, Spain.
Email: ribovi@doctor.upv.es

Funding information
Departamento Administrativo de Ciencia, Tecnología e Innovación COLCIENCIAS (Colombia) call, Grant/Award Number: 728-2015; Spanish Ministry of Science and Innovation through the research project TETISCHANGE, Grant/Award Number: RTI2018-093717-B-I00

Abstract

Flooding can destabilize vehicles which might, in turn, exacerbate the negative effects of floods when vehicles are swept away by flows, and lead to economic loss and fatalities. In order to suitably manage floods, it is necessary to determine the risk of instability to which vehicles in flood-prone areas are subject. This paper develops a methodology to estimate this risk based on the characteristics of floods and the vehicle fleet located in potential flood-prone areas. This risk is determined by the statistical integral of the instability hazard and vehicles' vulnerability. The instability hazard was established by a stability function of partially submerged cars and flood frequency, while vulnerability was calculated by combining the susceptibility and exposure of cars. Our methodology was applied in the towns of Alfafar and Massanassa (Spain). It found that the annualized instability risk due to flooding could be relatively high on most streets and roads, with values reaching the order of 8.4 at-risk vehicles per hectare/year.

KEYWORDS

floods, risk of vehicle instability, vehicle instability hazard, vehicle stability, vulnerability of vehicles

1 | INTRODUCTION

Floods are considered a natural phenomenon with a major impact on human activities compared to other natural threats (CEOS, 2003; CRED, 2017). The main damage caused by floods include loss of human life and economic loss, most of which are related to vehicles' security and them not being able to drive around flooded areas.

When rivers overflow, transport systems can be badly affected because traffic is interrupted given the risk for those vehicles driving around or parked on floodplains (Teo et al., 2012). As vehicles are shifted by flow, they can act as debris that can increase the negative impacts of flooding by impacting existing infrastructure and blocking hydraulic works (Pregnolato et al., 2017; Teo et al., 2012). In August 2010, flooding took place in the Spanish town of Águilas and dragged 15 cars, of which seven ended up in the sea, and eight hit walls and palm trees (Castejón & Romero, 2014). In April 2013, the flooding caused by rainfall, which reached 398 mm in just a few hours in the city of La Plata (Argentina), killed more 60 people, and flooded and dragged many vehicles (Cáneva, 2014). In May 2018 in Barranquilla (Colombia), the torrents of water brought by a precipitation episode exceeding 80 mm swept away more than 40 cars (El Tiempo, 2008).

During flood events, most casualties are caused by vehicles when drivers attempt to drive along flooded roads (Fitzgerald et al., 2010). In the United States, 45.4%

of the people who died during flooding had been inside vehicles (Jonkman & Kelman, 2005). Every year in Texas (USA), an average of 15 drivers drown when they drive their vehicles on flooded underground roads or through tunnels (Maples & Tiefenbacher, 2009). Between 2008 and 2018 in Spain, 125 cars were swept away during flood events and, as a result, 45 people died and 155 more were injured (Enríquez de Salamanca, 2020). Between 2001 and 2017 in Australia, 96 people lost their lives in 74 vehicle-related incidents during flooding (Ahmed et al., 2020).

Additionally, flooding of roads affects vehicles used by emergency services, such as ambulances and fire-fighters. The response times of these services can significantly be prolonged due to vehicles' inability to drive safely through flooded areas, which aggravates the negative impacts of floods (Arrighi et al., 2019; Coles et al., 2017; Green et al., 2017; Johnson & Yu, 2020).

Apart from fatalities, damaged infrastructure and interrupted traffic, and rescuing people trapped in their vehicles in flooded areas, demand costly investments in money and time terms. Moreover, as a result of climate change and growing urban development, such threats are expected to continue in the future (Xia et al., 2011). So for land management to be adequate, it is necessary to identify safe areas and the risk to which different vehicle types are exposed during floods.

Most published studies about vehicle instability risk have focused on determining the hazard or vulnerability of roads due to floods using the characteristics of basins and road networks. Some include the method of flood hazard maps proposed by Kalantari et al. (2014). This method allows the probability of flood hazards to be calculated by a multiple factor analysis, which considers topography, land use, soil texture, and roadway density. Michielsen et al. (2016) presented a methodology for identifying vulnerability caused by the flooding of a transport network based on the analysis of basin characteristics using statistical methods. Versini et al. (2010) reported a method to evaluate the susceptibility of roads being flooded using geographic information and statistical analysis methods based on general discriminant analysis principles.

Of the few studies that have attempted to really assess the flooding risk, we find the method set forward by Yin et al. (2016) to establish the risk of flash-floods on an urban roadway network. In this methodology, risk is determined through the integral of the multiplication of flood occurrence probabilities and their corresponding consequences, established with the combination of flooded road length and the time during which roads remain flooded. Pregnolato et al. (2017) developed a method to determine the impact of flooding on a transport network by means of a function that relates flood depth to interrupted traffic. This study establishes the interruption risk by means of the integral of the result of each rain event probability, multiplied by the expected interruption of traffic.

The present research presents a new methodology that determines the vehicle instability risk in urban areas as a result of overflowing rivers with a formal statistical basis to allow the number of at-risk vehicles per year to be established. Bearing this objective in mind, the mechanisms that cause a submerged vehicle to lose its stability are initially described. It then goes on to describe the methodology followed by indicating the process to be followed to calculate hazard, vulnerability, and the vehicle instability risk. It also presents how this methodology is implemented to determine the vehicle instability risk in the flood-prone areas of the towns of Massanassa and Alfafar, which lie south of Valencia (Spain) and very close to the Spanish Mediterranean coastline. Finally, it indicates the main conclusions drawn from developing the presented methodology and its corresponding implementation.

2 | VEHICLE STABILITY IN FLOODED AREAS

2.1 | Loss of vehicle stability

On a partially submerged vehicle, the forces of floating F_B, lift F_L, own weight W, drag F_D, and friction F_R act (Arrighi et al., 2015; Martínez-Gomariz et al., 2017; Milanesi & Pilotti, 2019; Oshikawa and Komatsu, 2014; Toda et al., 2013). The action of all these forces gives way to three hydrodynamic mechanisms to come into play, which can destabilize a vehicle: floating, sliding, and toppling. Stability loss due to floating occurs when forces floating F_B and lift F_L exceed the vehicle's weight (W) (Shand et al., 2011). This destabilization mainly takes place when flow presents great water depths and slow velocities. As engines in today's vehicles sit at the front of vehicles, initially the rear vehicle part mostly floats. Then the vehicle spins and is supported on its front wheels, and is mobilized by flow in most cases.

Vehicle destabilization caused by sliding takes place when drag force F_D, generated by flow, exceeds friction force F_R, which depends on the friction coefficient between the vehicle's tire rims and the wet surface (Smith et al., 2019). An interaction takes place between the floating and sliding mechanisms because both forces lift F_L and floating F_B that lower normal force F_N which, in turn, lowers friction force F_R.

Destabilization owing to the vehicle toppling may take place when vehicles have already been swept away

or floated before finding irregular ground (Shand et al., 2011). This mechanism has been poorly studied to date.

2.2 | Determining vehicle instability index

To calculate vehicle instability conditions, a criterion needs to be defined to establish when the depth and velocity of flows corresponding to different return period floods generate vehicle instability, which also depends on the characteristics of each vehicle type.

To date, very few studies have attempted to determine vehicle stability during floods, and some date back to the 1960s, 1970s, and 1990s. However, their results are no longer valid because vehicle characteristics have changed with time (Suárez et al., 2005; Teo et al., 2012). Some models have been recently developed to determine vehicle stability during floods and are based on the vehicle-flow interaction analysis (e.g., Austroads, 2008; Teo et al., 2012). A compilation and analysis of the presently available methodologies are presented by Bocanegra et al. (2020).

The present study selected the stability model developed by Arrighi, Castelli, and Oumeraci (2016) and Arrighi, Huybrechts, et al. (2016), because it is considered one of the most robust methodologies of those proposed in scientific literature (Bocanegra et al., 2020) for these reasons: (i) the equations that it contemplates have a solid theoretical basis; (ii) it considers the Froude number, which is a very important and widely used parameter in many formulations; (iii) it allows vehicles' watertightness and nonwatertightness conditions to be taken into account; (iv) it enables stability to be determined for any vehicle type.

From the balance of horizontal forces that acts on type i car located on a plane at a slope of zero, and based on the diagram provided in Figure 1, Arrighi, Castelli, and Oumeraci (2016) and Arrighi, Huybrechts, et al. (2016)) defined the following mobility parameter θ_{vi}:

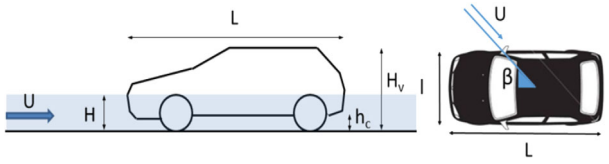

FIGURE 1 Geometry of the car used to determine mobility parameter θ_v. *Source:* Arrighi, Castelli, and Oumeraci (2016) and Arrighi, Huybrechts, et al. (2016)

$$\theta_{v_i} = \frac{2L}{(H_v - h_c)} * \frac{l}{l * \mathrm{Cos}\beta + L * \sin\beta} * \left(\frac{\rho_c * (H_v - h_c)}{\rho * (H - h_c)} - 1 \right), \tag{1}$$

where ρ_c is the car's mean density, ρ is water density, h_c is the distance between the chassis and the ground, H is the undisturbed water depth, β is the angle of flow incidence, and H_v, L, and l are car height, car length, and car width, respectively.

Mobility parameter θ_{vi} is defined for the water levels reaching the chassis and is made up of three factors: the first factor 2 L/($H_v - h_c$) bears in mind the car's shape; the second considers the angle of flow incidence; the third factor takes into account the submerged weight in relation to the car.

Mobility parameter θ_{vi} was calculated by Arrighi, Castelli, and Oumeraci (2016) and Arrighi, Huybrechts, et al. (2016) with the experimental data reported by Shu et al. (2011) and Xia et al. (2011, 2014), which included measures taken in seven car models on scales 1:14, 1:18, and 1:43. The obtained results allowed critical mobility parameter θ_{vcr} to be obtained, which can be established by the equation below,

$$\theta_{vcr} = 8.2\,Fr^2 - 14.1\,Fr + 5.4, \tag{2}$$

where Fr is the Froude number, which requires data only about water depth H and velocity U. This means that a vehicle instability index, S_i, can be defined as the relation between critical mobility parameter θ_{vcr} (defined in Equation (2)) and mobility parameter θ_{vi} for this vehicle (defined by Equation (1)),

$$S_i = \frac{\theta_{vcr}}{\theta_{V_i}}. \tag{3}$$

The interesting point about this index is that different vehicle stability or instability situations can be found depending on the value they take: if $S_i \geq 1$, then the vehicle will destabilize due to sliding; if $S_i < 0$, the vehicle will float; if $0 \leq S_i < 1$, the vehicle will remain stable. Also, it should be noted that the higher the Froude number, the more dangerous the flow is for vehicles because lower water depth values are required to destabilize them.

3 | METHODOLOGY TO ESTIMATE THE VEHICLE INSTABILITY RISK USING FORMAL STATISTICS

In general, risk is determined by integrating hazard and vulnerability, and established by combining exposure

and susceptibility. In the specific case of the vehicle instability risk from flooding, the hazard corresponds to the probability of the vehicle being dragged or it floating, exposure is established by the types and density of vehicles at a given point of the territory located in flood-prone areas, and susceptibility is determined by the capacity or incapacity of the vehicle remaining stable. Susceptibility is expressed with a damage function, which in this case takes a value of 0 when the vehicle remains stable and 1 when the vehicle loses its stability.

Generally speaking, risk corresponds to the expected annual damage. In this methodology, instability risk, R, at a specific point is defined as the mean number of vehicles that would destabilize annually per unit area. In line with Hashimoto et al. (1982), this risk can be calculated at a given point on the territory by employing the following statistical integral that was adapted to this problem:

$$R = \int_0^1 V(s_i)\, dF_{s_i} = \int_0^\infty V(s_i) f_{s_i}(s_i) ds_i, \qquad (4)$$

where $V(S_i)$ is vulnerability, calculated by combining the damage function and exposure to an event of magnitude S_i, which was defined in previous subsection; F_{Si} is the cumulative distribution function of S_i; and f_{Si} is its probability density function. The following subsections describe the procedure that must be set up to calculate the risk and all its components.

3.1 | Vehicle instability hazard

To calculate the vehicle instability hazard, information is required about the flooding hazard (which can be defined as the combination of its magnitude and its frequency of occurrence), along with vehicles' physical characteristics. Flood magnitude is usually established with maximum flow water depth and its corresponding velocity. A similar graph to that in Figure 2(a) can be obtained when graphically representing the occurrence of each flood event against its magnitude at a point of the floodplain.

The flood hazard is normally represented on maps with its maximum water depth h and its corresponding velocity u for different return periods. With the information depicted on these maps, instability index S_i is calculated for every vehicle i at each point of the territory using Equation (3). When graphically representing the magnitude of each flood event against its corresponding

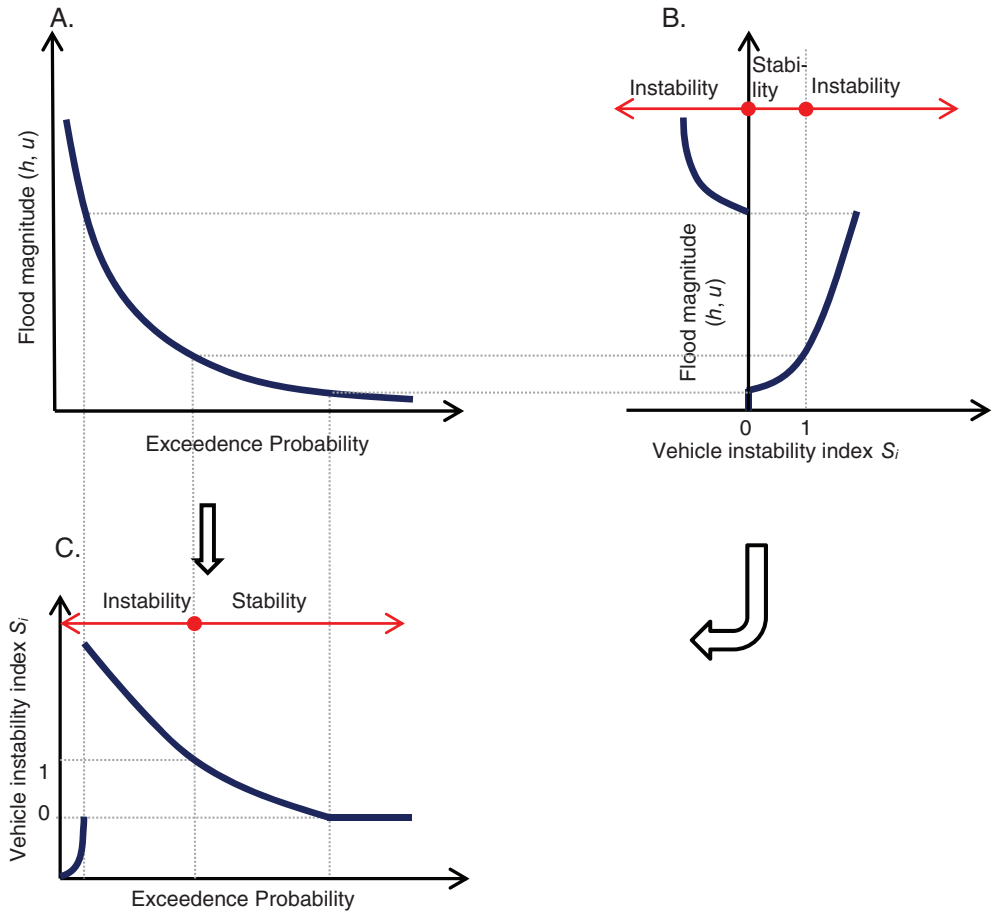

FIGURE 2 Diagram illustrating the process that must be implemented to calculate the instability hazard in one vehicle i

S_i, a similar graph to that shown in Figure 2(b) is obtained. Finally, the graphical representation of the exceedance probability of all flood events against their corresponding S_i provides a similar figure to that seen in Figure 2(c), which depicts the vehicle instability hazard at a given point of the floodplain. In other words, the vehicle instability hazard can also be represented on vehicle instability index S_i maps for each return period as the flood magnitude.

3.2 | Vulnerability

Vulnerability represents the characteristics of a system that describes its damage potential (Samuels et al., 2009; UNISDR, 2009), which is calculated by combining exposure and susceptibility. Exposure for one vehicle type i is calculated by multiplying vehicle spatial density d at a point of interest by the proportion g_i of this type of vehicle in the vehicles fleet in the study area. In order to calculate the flood susceptibility of one vehicle of type i at a given point, damage function $D(S_i)$ must be established using vehicle instability index S_i. The objective of this paper is the vehicle instability risk. For this reason, when vehicle is unstable (i.e., when vehicle instability index S_i takes negative values or values equaling or exceeding 1), the damage function takes a value of 1, which means that 100% damage has taken place. When the vehicle remains stable (i.e., when the instability index takes positive values below 1), the damage function takes a value of 0, which means that the vehicle is not damaged (Bocanegra and Francés, 2021). In mathematical terms, this damage function is defined as follows:

$$D(S_i) = \begin{cases} 0 \text{ if } 0 \le S_i < 1 & \text{(stable vehicle)} \\ 1 \text{ otherwise} & \text{(unstable vehicle)} \end{cases}. \quad (5)$$

Finally, the vulnerability $V(S_i)$ of type i vehicles at a given point of interest is calculated by this equation:

$$V(s_i) = d\, g_i\, D(s_i). \quad (6)$$

3.3 | Vehicle instability risk

The instability risk is determined by Equation (4). When substituting Equation (6) in Equation (4), and bearing in mind the different vehicle types, the following expression is obtained:

$$R = \sum_{i=1}^{K} d\, g_i \int_0^1 D(s_i)\, dF_{S_i} = \sum_{i=1}^{K} d\, g_i \int_0^\infty D(s_i) f_{S_i}(s) ds, \quad (7)$$

where K corresponds to the number of vehicle types by means of which the whole fleet is represented.

Figure 3 presents a diagram of the procedure that must be followed to calculate the instability risk of a vehicle type i at a point on the territory. Panel (a) corresponds to the instability hazard, which is calculated as described in Figure 2. Panel (b) presents the damage function, as calculated in Equation (5). When the instability hazard is combined with damage function $D(Si)$, each probability of a flood event happening takes a certain damage function value. When graphically representing the probability of each flood event against the corresponding damage function values, a similar graph to that found in panel (c) is obtained, and the instability risk for a vehicle type i at a point on the territory corresponds to the area under this curve.

As previously mentioned, vehicle instability hazard is represented on vehicle instability index S_i maps and each S_i has a corresponding damage function $D(S_i)$ value. Accordingly, the value of this function between two flood events with return periods T_j and T_{j-1}, respectively, is obtained by defining a new function known as $D(S_{i,j})$, which is calculated by averaging the damage function $D(S_i)$ values corresponding to the two superior and inferior events in terms of T. By bearing this in mind, the following expression is obtained when discretely solving Equation (7):

$$R = \sum_{i=1}^{K} d\, g_i \sum_{j=T\min}^{N} \bar{D}(s_{i,j}) \left(\frac{1}{T_{j-1}} - \frac{1}{T_j} \right), \quad (8)$$

where j corresponds to the flood hazard map for return period T_j and $T_{\min}$ corresponds to the lowest return period from which flooding commenced.

The $T_{\min}$ concept is introduced into Equation (8). As the flood events with a relatively low return period have a much stronger effect on the final risk values than the less frequent events, determining the value of return period $T_{\min}$ is particularly important because any mistakes or inaccuracies in this value might involve over- or underestimating the risk. The impact of $T_{\min}$ on the risk values is illustrated in the sensitivity analysis of the case study in the next section (section 4.7).

4 | CASE STUDY

In order to verify the procedure's applicability to a real case, to analyze the validity of the obtained results and to determine their sensitivity to $T_{\min}$, the developed methodology was implemented to establish the vehicle instability risk in the Spanish towns of Massanassa and Alfafar, which are located in the floodplain of Rambla del Poyo.

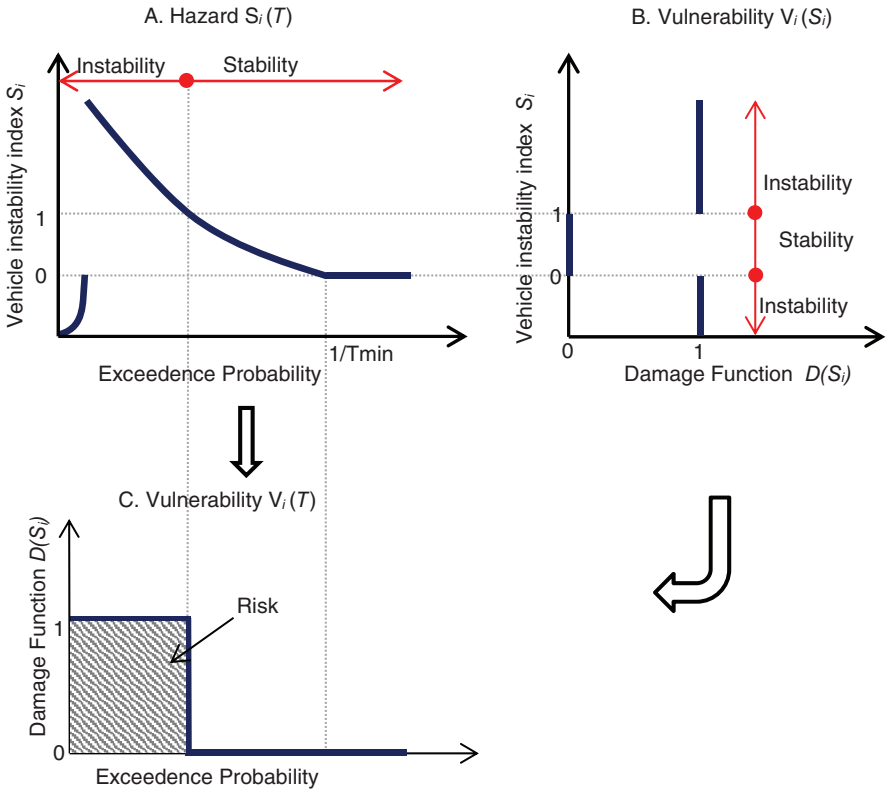

FIGURE 3 Diagram of the instability risk of a single vehicle type *i*

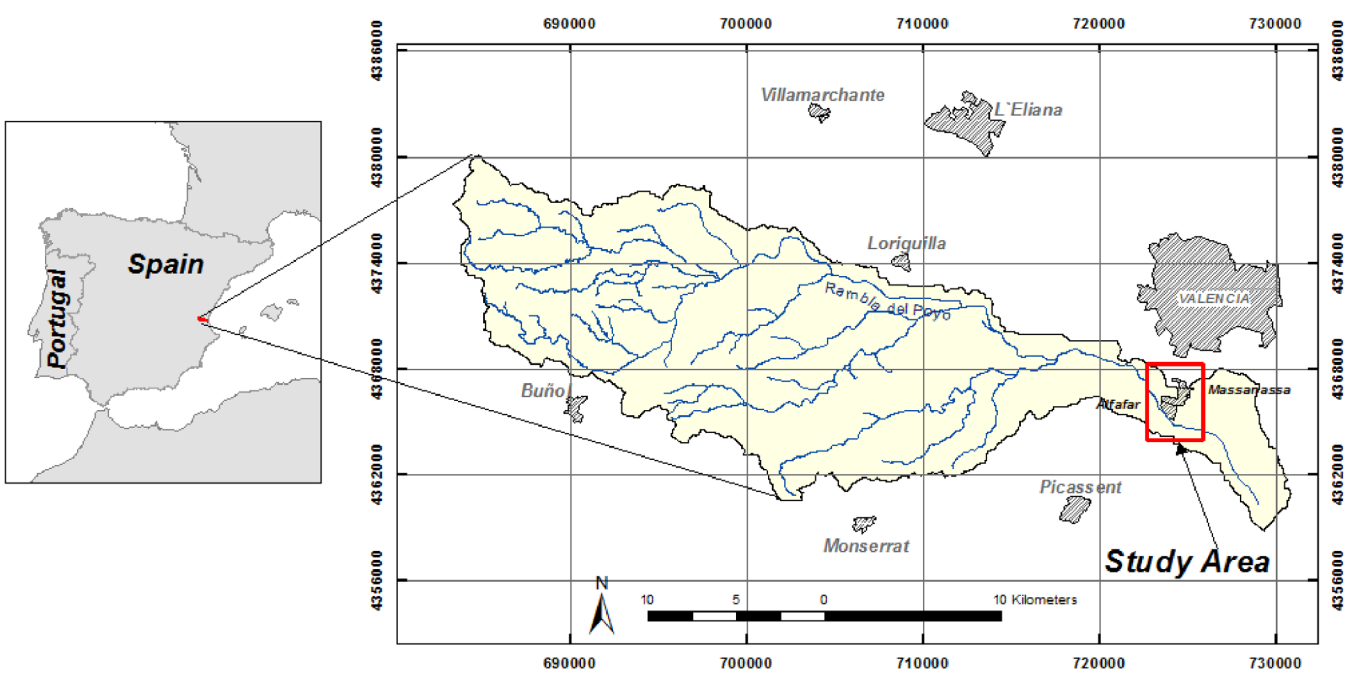

FIGURE 4 Location of the Rambla del Poyo basin and the study area

4.1 | Description of the study area

Rambla del Poyo is an intermittent watercourse located in the province of Valencia (east Spain). It flows into the Albufera coastal lagoon, and its basin covers 430 km^2 (Figure 4). The climate is classified as semiarid Mediterranean, with mean annual rainfall of 450–500 mm, intense autumn and spring rainfall, and low winter and summer rainfall values. The basin's slope ranges between values over 16% in the high part and below 2% in the low

part. The configuration of the network of riverbeds favors the rapid concentration of flows upstream, followed by retarded flows in the main watercourse. Rambla del Poyo is characterized by flash floods with very marked hydrogram peaks and short baseline times (Salazar et al., 2012).

Areas affected by flooding are mainly located in low parts of the basin where less pronounced slopes predominate. They include the towns of Massanassa and Alfafar. Land use is residential in these towns. Shops and services occupy ground floors, especially in the blocks close to their town squares.

4.2 | Characterization and exposure of the vehicles in the study area

The proportion of vehicles by their type in the study area was established with the data published in 2018 by the Spanish Association of Manufacturers of Automobiles and Trucks (ANFAC, 2018):

1. Smaller cars, with 26% of the total. This vehicle type was represented by the car model Seat Ibiza.
2. Compact vehicles, with 32% of the total. This vehicle type was represented by the car model Seat León.
3. Small SUVs, with 15% of the total. This vehicle type was represented by the car model Peugeot 2008.
4. Medium-sized SUVs and larger vehicles, with 27% of the total. This vehicle type was represented by the car model Volkswagen Tiguan.

Table 1 presents the main characteristics of these vehicles. According to Francés et al. (2008), and by considering both parked vehicles and moving traffic, the vehicle spatial density in the study area is 0.005446 vehicles/m^2 in urban non built-up areas, and 0.0313 vehicles/m^2 of the street in urban built-up areas. The higher vehicle density in streets is explained by the high number of parked cars in streets.

4.3 | Vehicle stability thresholds

First, the vehicles' stability thresholds of the four vehicle types representing the vehicle fleet were determined. With the physical characteristics of these vehicles, and by employing Equations (1)–(3), the velocity from which every vehicle would lose its stability was calculated for each water depth. The obtained results are shown in Figure 5. The part of the graph over the threshold of each vehicle corresponds to the unstable zone; that is, the area where vehicles would destabilize. The part of the graph below the threshold corresponds to the stable zone; that is, the area where vehicles would remain stable.

The analysis of this graph indicated that the thresholds of the bigger vehicles exceeded those of the smaller vehicles; that is, for a given water depth, bigger-sized cars would remain stable at faster velocities than at the velocities guaranteeing smaller cars' stability. As expected, this meant that larger vehicles would be more stable during flooding.

At fast flow velocities, the water depths at which vehicles would destabilize displayed asymptotic behavior and came close to the clear distance value between the chassis and the ground. For slow velocities, the water depths that brought about vehicle destabilization tended to move closer to the values at which the vehicle would float under conditions when water was still.

4.4 | Vulnerability

As previously indicated, the two vulnerability components were represented by exposure and susceptibility. Exposure was determined by the proportion of each

TABLE 1 Characteristics of the vehicles in the study area

Characteristic	Type of vehicle *i*			
	Smaller cars *Seat Ibiza*	**Compact vehicles** *Seat León*	**Small SUVs** *Peugeot 2008*	**Medium-sized SUVs and larger vehicles** *Volksw. Tiguan*
Length (m)	3.68	4.18	4.16	4.43
Width (m)	1.61	1.74	1.74	1.81
Height (m)	1.42	1.44	1.56	1.67
Clear distance from ground (m)	0.12	0.12	0.17	0.18
Density (kg/m^3)	108.00	125.86	104.41	115.26
Proportion g_i (%)	26	32	15	27

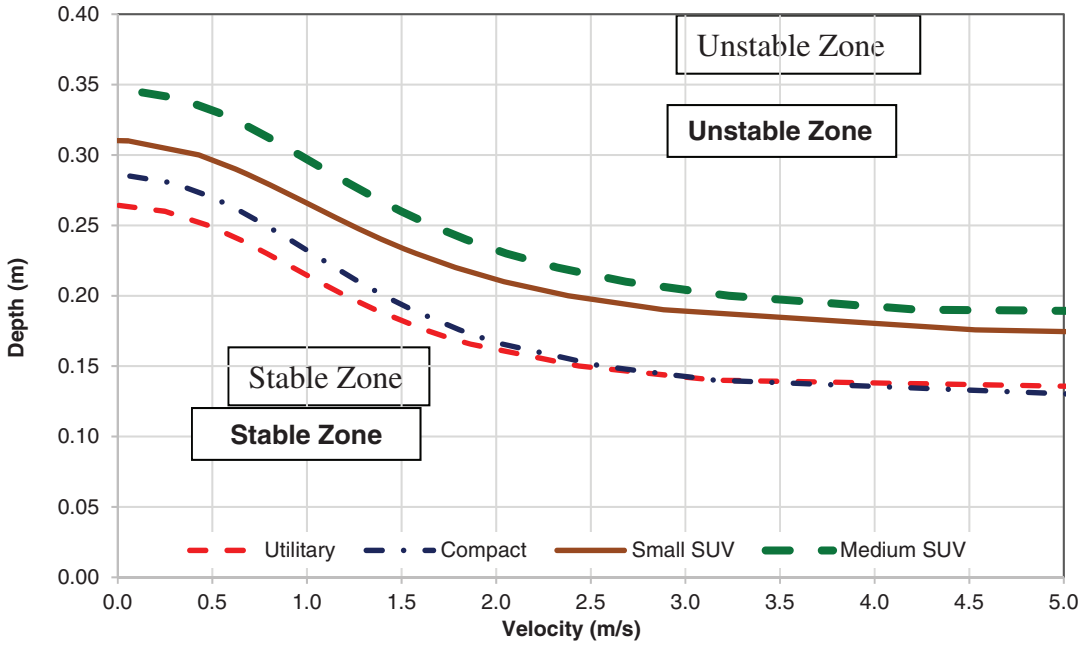

FIGURE 5 Stability thresholds for each vehicle type

vehicle type in fleet g_i (Table 1), and by vehicle density d, which took different values for urbanized areas that had and had not been built-up (see section 4.2). With these density values, the total number of vehicles driving around and/or parked in the flooded areas for the flood swell with a 500-year period equaled 18.205.

Susceptibility was established with the damage function, which was calculated using the vehicle instability index S_i values (see section 3.2). For a better spatial representation, and to facilitate their interpretation, on the hazard maps obtained for each studied vehicle type, these vehicle instability indices were divided into the following ranges according to stability: (a) range 1: indices below zero corresponding to the sectors in which vehicles would lose stability due to floating; (b) range 2: indices between 0.0 and 0.5 denoting that vehicles would probably remain stable; (c) range 3: indices between 0.5 and <1.0 meaning that vehicles would probably remain stable, but would be about to destabilize owing to the sliding phenomenon; (d) range 4: indices between 1.0 and 1.5 corresponding to the sectors in which vehicles would destabilize owing to the sliding phenomenon; (e) range 5: indices >1.5 representing those sectors in which vehicles would greatly destabilize owing to the sliding phenomenon.

According to Equation (5), damage function $D(S_i)$ takes a value of 1 when the hazard index has negative values (range 1), and equals or exceeds 1 (ranges 4 and 5). The damage function value equals 0 (ranges 2 and 3) in all the other cases.

Finally, the vulnerability for vehicles type i at a point on the territory was calculated by multiplying the proportion of a vehicle type in the fleet, gi, by vehicle spatial density, d, and by the damage function value, $D(Si)$, as set out in Equation (6).

4.5 | Vehicle instability hazard

The collected flood hazard data were provided by the Confederación Hidrográfica del Júcar (Júcar Hydrographic Confederation (CHJ), 2011), which employed the model Infoworks 2D to calculate the levels and velocities of flow in the flooded area. The flood hazard maps corresponding to those floods with return periods of 10, 25, 50, 100, and 500 years were available. The floods with return periods of 10 and 25 years did not affect the study area. This was why a $T_{\min}$ value equaling 37.5 years was defined, which corresponds to the average between the highest return period with available data for which the study area is not flooded (25 years), and the lowest return period with available data for which the study area is flooded (50 years).

Figure 6 presents the maximum water depth maps and their corresponding flow velocities for the flooding with the 100-year return period. It can be highlighted that for some sectors of the study area, the flow depths for this event exceeded 4.0 m (Figure 6(a)) and velocities went over 3.0 m/s (Figure 6(b)).

The vehicle instability hazard was calculated by Equation (3) and the procedure is graphically represented

in Figure 2. As the vehicles representing the vehicles fleet presented different characteristics, a hazard map can be calculated for each vehicle type and all the analyzed floods. In order to determine vehicle instability index S_i, it was assumed that cars were completely watertight and lay perpendicularly to the flow, which usually represents the most unfavorable condition because the cross-sectional area exposed to the flow and, consequently, the hydrodynamic force applied to vehicles are maximized (Smith et al., 2017).

By way of example, Figure 7 presents the hazard maps of vehicle instability obtained for Seat Ibiza (represents smaller vehicles) by considering floods with return periods of 50 and 500 years. In most flooded areas, the vehicle instability index values were below 0.5 and negative values predominated. A similar behavior was noted on the other instability hazard maps created for the other vehicle types and return periods.

The analysis done with the results for all the vehicles and return periods indicated that the Rambla del Poyo floods with return periods over 50 years would pose a major hazard for all the vehicles, because even bigger vehicles would lose their stability in most flooded areas ($S_i < 0$ or $S_i \geq 1$). With medium-sized SUVs and larger vehicles, represented by Volkswagen Tiguan, both water depths and flow velocities would destabilize these vehicle

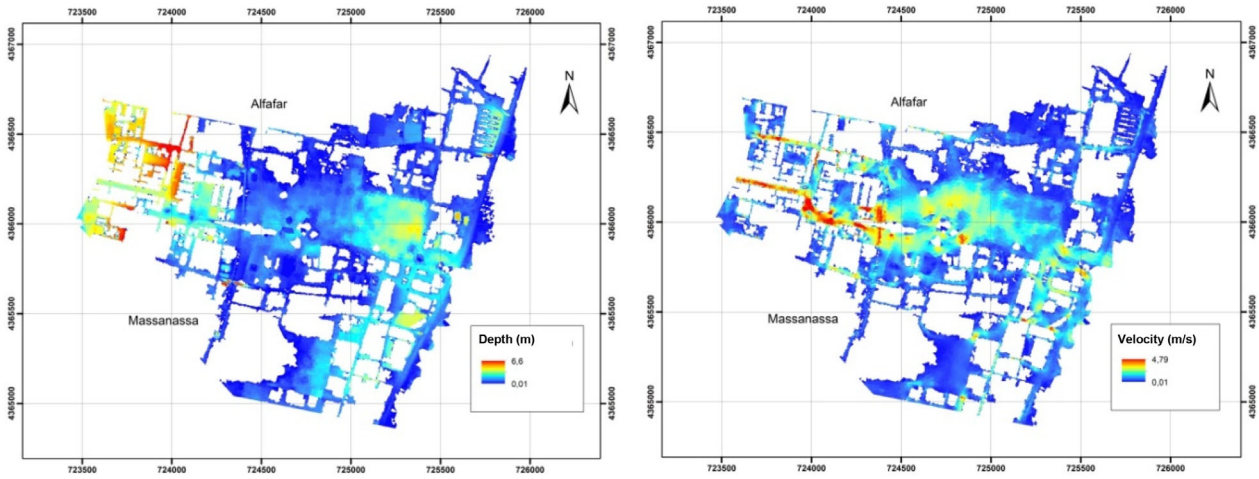

FIGURE 6 Flood hazard: maximum water depths and their corresponding flow velocities in the study area due to the la Rambla del Poyo flooding with a 100-year return period. *Source:* Confederación Hidrográfica del Júcar (2011)

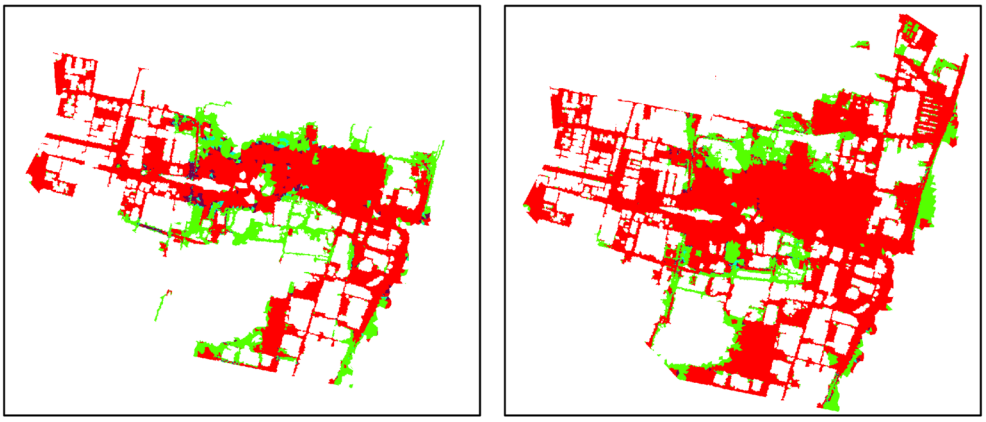

FIGURE 7 Hazard maps of vehicle instability in the study area for floods with return periods of 50 and 500 years for Seat Ibiza

types in 66% of the flooded areas due to flooding with a 50-year return period. This percentage would rise to 74% if the behavior of smaller cars (represented by Seat Ibiza) was evaluated during the same event. When considering a flood with a 500-year return period, the percentages of areas in which vehicles would destabilize would rise to 76% for medium-sized SUVs, and up to 80% for smaller vehicles.

As a result of the high flow depth values shown in most of the flooded zones in the study area, loss of stability of all the studied vehicle types would be mostly attributed to the floating phenomenon ($S_i < 0$), while the sliding phenomenon would have less impact ($S_i \geq 1$). For instance with smaller vehicles, as the corresponding floods would present a 500-year return period (Figure 7 (b)), the floating phenomenon would cause vehicle destabilization in 79% of the flooded areas, whereas the sliding phenomenon would do so in only 1% of these areas. Similar behavior to this was observed for the remaining return periods and other vehicle types.

The high percentage of the areas in which vehicles would lose their stability due to the floating phenomenon is associated with the areas in which high flow depths occur (see Figure 6(a) for 100-year return period). This situation is very dangerous for people because, apart from the risk of vehicle instability, their stability can be compromised when leaving the vehicle, which also makes rescue activities difficult for the institutions in charge of them.

It is worth pointing out that in percentage terms, the flooded areas that were safe for vehicles lowered as flooding frequency reduced and flooding magnitude rose. For example with smaller vehicles (Seat Ibiza), for flooding with a 50-year return period, 104 hectares (ha) would be flooded and cars would remain stable in 28% of them. However for the flooding with the 100-return period, 174 ha would be flooded and vehicles would remain stable in only 26% of them. For the flooding with a 500-year return period, 193 ha would be flooded and vehicle stability would remain in only 20%.

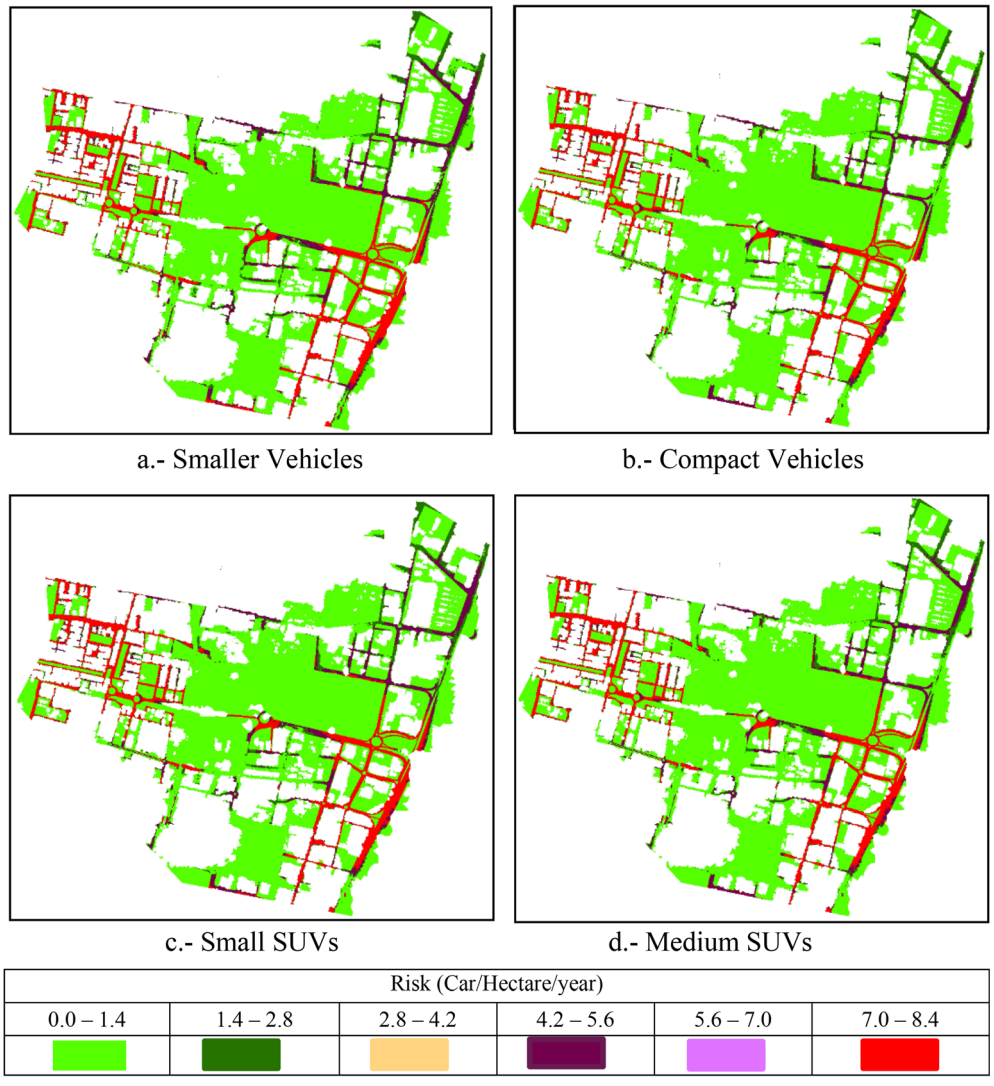

FIGURE 8 Risk map of instability for each vehicle type studied in the study area without considering their proportion in the vehicle fleet

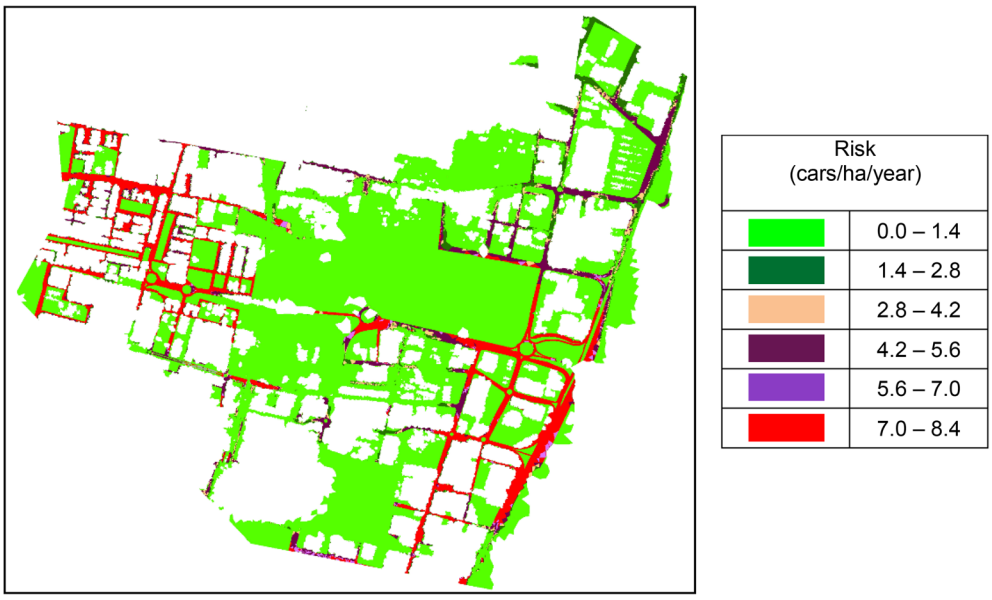

FIGURE 9 Map of the instability risk for vehicles in the study area

As expected, and in accordance with Figure 5, given their bigger size and the greater clearence between their chassis and the ground, medium-sized SUVs (the biggest vehicle type herein included) would be the safest, because they would remain stable in larger-sized flooded areas than the other vehicle types. But not everywhere. Which is true is that the size of the flooded areas in which vehicles would conserve their stability would progressively reduce with vehicle size until their lowest area for smaller vehicles.

4.6 | Vehicle instability risk

The instability risk for each vehicle type was calculated by Equation 8 and the procedure depicted in Figure 3. The instability risk maps obtained for each employed vehicle type are shown in Figure 8 without considering their proportion in the vehicle fleet. The analysis of these maps indicated that as vehicle size increased, the areas with a higher instability risk (streets) diminished and, consequently, the low-risk areas increased. This result was expected because, as indicated in section 4.5, the bigger the car size, the greater its stability during floods.

Figure 9 shows the aggregated risk map of instability, which was obtained by summing the risk maps of each vehicle type, multiplied by their proportion in the vehicle fleet. It is noteworthy that in streets, where vehicle density exceeded the density of all the other urban areas by almost 6-fold, the instability risk obtained the highest values (of the order of 8.4 cars/ha/year). These relatively high-risk areas corresponded to about 8% of the whole flooded area. Otherwise, in an area that roughly equaled 60% of the flooded area, the risk for vehicles was relatively low, with values below 1.4 cars/ha/year.

TABLE 2 Mean annual number of at-risk vehicles for instability in the whole study area in line with the two fleet hypotheses: only one type and with the present proportion

	Mean annual number of at-risk vehicles	
	Representation of the fleet	
Vehicle type	A single vehicle type	The four vehicle types and their proportions
Smaller vehicles	276.5	71.9
Compact vehicles	269.7	86.3
Small SUVs	252.7	37.9
Medium-sized SUVs and larger vehicles	244.1	65.9
Total	–	262.0

Table 2 shows the annual number of cars at risk of being dragged by the flood flow according to two hypotheses: (i) the vehicle fleet was represented by a single vehicle type (column 2); (ii) the vehicle fleet was represented by all four vehicle types indicated in section 4.2 (column 3). When the data in column 2 were analyzed, once again it was concluded that bigger vehicles (i.e. medium-sized SUVs) were the most stable vehicle type during flooding as they posed fewer at-risk vehicles for instability. The smaller vehicles (Seat Ibiza) were the least stable cars by presenting the most at-risk number of vehicles.

By analyzing the data in column 3, it was concluded that compact vehicles (i.e., Seat León) posed the highest

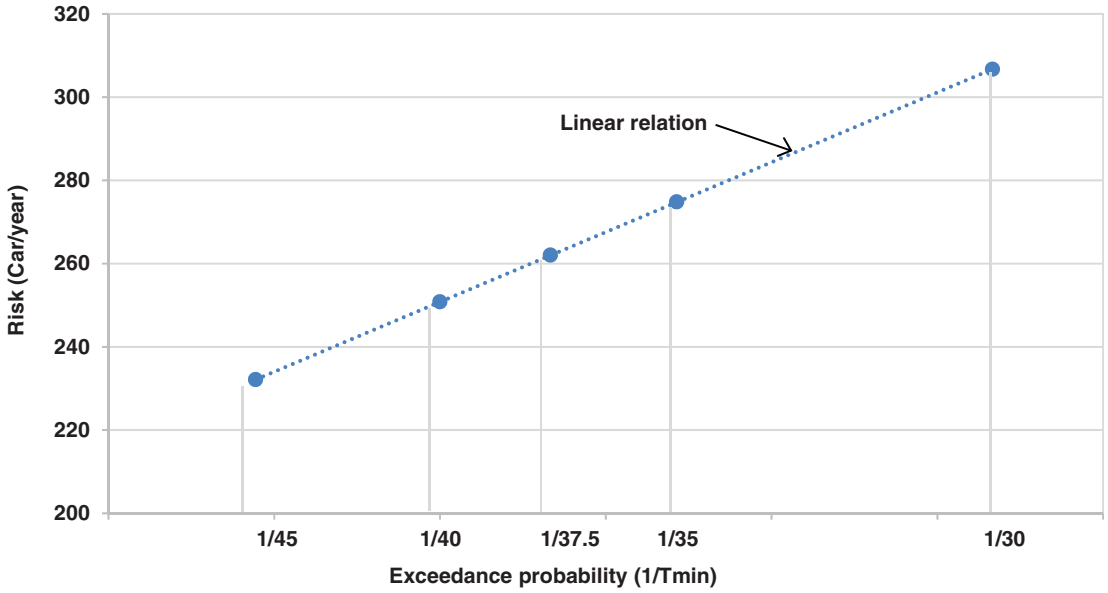

FIGURE 10 Number of cars at risk of instability in the study area when considering different T_{min} values

risk, which corresponded to roughly one third of all the at-risk vehicles. This was because, despite not being the most unstable cars, they had the highest proportion in the vehicle fleet. Smaller (least stable) vehicles presented a slightly lower risk than compact vehicles as their proportion in the vehicle fleet was also lower. The vehicles with the lowest instability risk in the study area corresponded to small SUVs because they were one of the most stable vehicle types with the lowest proportion in the vehicle fleet compared to the other studied vehicle types. For this reason, this vehicle type only represented about 15% of all the at-risk vehicles.

4.7 | Sensitivity analysis to T_{min}

Bearing in mind the uncertainty for the return period value from which the study area started being flooded (known in this methodology as T_{min}), the sensitivity of the vehicle instability risk to the values of this variable should be determined. According to available flood maps, as the 25-year return period flood envelope does not reach the study area, unlike the 50-year return period flood which does, the potential T_{min} values adopted were 30, 35, 40, and 45 years, plus 37.5 years, which was the value employed to implement the methodology.

Figure 10 offers the results for this relatively simple sensitivity analysis. The conclusion drawn from studying this graph was that a linear relation appeared between the exceedance probability of the event corresponding to T_{min}, which equals $1/T_{min}$, and the number of at-risk vehicles; the higher the probability of the event considered to be T_{min} occurring, the more the at-risk vehicles. Furthermore, T_{min} significantly influenced vehicles' instability risk values. In relation to the value taken for the methodology implementation, the number of at-risk vehicles dropped by approximately 12% when taking a 45-year T_{min} value, and rose by about 17% when a 30-year T_{min} value was taken.

5 | CONCLUSIONS

This paper developed a methodology that allows the estimation of vehicle instability risk during flooding, while being driven or parked at a given point on the territory. This methodology estimates the annualized mean number of at-risk cars by classifying these by vehicle type and being representative of the vehicle fleet in any given area.

Efforts were made to develop a rigorous methodology from the statistical point of view, but at the same time one that is relatively simple to implement. To determine the vehicle instability risk, it is only necessary to have the maximum water depths and flow velocities of floods for some return periods, as well as the basic characteristics of the vehicles in this area. The instability hazard is determined according to a stability function of partially submerged vehicles. Vehicles' vulnerability is established by combining exposure and susceptibility: exposure is calculated by multiplying vehicle density by each vehicle's proportion in the fleet; susceptibility is determined with the damage function, which takes values of 0 (unharmed vehicles) and 1 (100% vehicle damage) depending on whether the vehicle is stable or not.

Finally, the risk at each point is obtained by adopting a numerical approximation of the statistical integral of the instability hazard and vehicles' vulnerability.

The number of vehicles at flood risk can be sensitive to the return period corresponding to the event in which the area of interest starts to flood, which is known as $T_{\min}$ in this methodology. A more precise estimate of this return period would allow obtaining more real values for at-risk vehicles. Also, the representation of the vehicle fleet in the flood-prone area significantly influences the overall value of the vehicles at risk for instability. Therefore, any mistaken or inaccurate selection of the vehicles that represent the vehicle fleet may distort the results.

One of the hypothesis in this research considers constant vehicle densities over time during flood events for both parked and moving vehicles. However, the traffic is dynamic and drivers can avoid areas that are flooding. Accordingly, the present methodology can be improved by considering the effect that the traffic variations may have on the vehicle spatial density during the flood event.

Applying the methodology to the selected case study allowed us to observe that the Rambla del Poyo floods with return periods of 50 years or longer are a major hazard for the vehicles located in the study area because they would destabilize in most of the flooded area. The most damaging effect would result from the vehicle floating phenomenon owing to the vertical ascending pushing caused by flows from overflowing rivers, which would present relatively high water depth values. Loss of vehicle stability owing to the sliding phenomenon would occur in relatively small areas.

The vehicle instability risk due to flood events in the towns of Massanassa and Alfafar is relatively high in their streets, with an estimated value of about 8.4 destabilized cars per ha/year. Larger vehicles (medium-sized SUVs) would be the most stable vehicle type, while smallest vehicles, represented by smaller vehicles type, would be the least stable. Nonetheless, given the actual fleet proportions in this case study, the vehicle type at highest risk is compact cars, whereas the vehicle type at lowest risk is small SUVs.

The developed methodology provides a detailed spatial vision of the vehicle instability risk due to flooding in a given area. The resulting maps allow to accurately locating not only the areas of higher risk for vehicles (for both each vehicle type and for the entire existing vehicle fleet), but also the safe ones. Consequently, implementing this methodology can help to reduce negative effects before and during flooding events, which is extremely helpful for those organizations in charge of urban planning and civil protection to design and take actions that mitigate the negative effects of flooding.

ACKNOWLEDGMENTS

This work was supported by Departamento Administrativo de Ciencia, Tecnología e Innovación COLCIENCIAS call 728-2015 (Colombia) and by the Spanish Ministry of Science and Innovation through research project TETISCHANGE, Grant/ Award Number RTI2018-093717-B-I00.

DATA AVAILABILITY STATEMENT

The data that support the findings of this study are openly available in http://www.anfac.com/estadisticas.action.

REFERENCES

Ahmed, M. A., Haynes, K., & Taylor, M. (2020). Vehicle-related flood fatalities in Australia, 2001–2017. *Journal of Flood Risk Management*, *13*(3), e12616. https://doi.org/10.1111/jfr3.12616

ANFAC. (2018). *Spanish association of truck and automobile manufacturers*. Retrieved from http://www.anfac.com/estadisticas.action

Arrighi, C., Alcérreca-Huerta, J., Oumeraci, H., & Castelli, F. (2015). Drag and lift contribution to the incipient motion of partly submerged flooded vehicles. *Journal of Fluids and Structures*, *57*, 170–184. https://doi.org/10.1016/j.jfluidstructs.2015.06.010

Arrighi, C., Castelli, F., & Oumeraci, H. (2016). Effects of flow orientation on the onset of motion of flooded vehicles: Proceedings of the 4th IAHR Europe Congress (Liege, Belgium, 27–29 July 2016). In *Sustainable hydraulics in the era of global change* (pp. 837–841). CRC Press. https://doi.org/10.1201/b21902-140

Arrighi, C., Huybrechts, N., Ouahsine, A., Chaseé, P., Oumeraci, H., & Castelli, F. (2016). Vehicles instability criteria for flood risk assessment of a street network. *Proceedings of the IAHS*, *373*, 143–146. https://doi.org/10.5194/piahs-373-143-2016

Arrighi, C., Pregnolato, M., Dawson, R. J., & Castelli, F. (2019). Preparedness against mobility disruption by floods. *Science of the Total Environment*, *654*, 1010–1022. https://doi.org/10.1016/j.scitotenv.2018.11.191

Austroads. (2008). *Guide to road design, part 5: Drainage design*. AusRoads Inc.

Bocanegra, R. A., & Francés, F. (2021). Determining the vehicle instability risk in stream crossings. *J Flood Risk Management*, *14*, e12737. https://doi.org/10.1111/jfr3.12737.

Bocanegra, R. A., Vallés-Morán, F. J., & Francés, F. (2020). Review and analysis of vehicle stability models during floods and proposal for future improvements. *Journal of Flood Risk Management*, *13*(suppl 1), e12551. https://doi.org/10.1111/jfr3.12551

Cáneva, V. (2014). Reemergencia de ciudadanía en momentos de crisis eco-ambientales y político sociales: una mirada comunicacional sobre las organizaciones de vecinos autoconvocadas post inundación en la ciudad de la plata. In *Proceedings of ALAIC 2014*. ALAIC.

Castejón, P. G., & Romero, D. A. (2014). Inundaciones en la región de Murcia en los inicios del siglo XXI. *Revista bibliográfica de geografia y ciencias sociales*, *XIX*, 1–40.

Centre for Research on the Epidemiology of Disasters (CRED). (2017). *Annual disaster statistical review 2016 the numbers and trends*. Université catholique de Louvain.

Coles, D., Yu, D., Wilby, R. L., Green, D., & Herring, Z. (2017). Beyond "flood hotspots": Modelling emergency service accessibility during flooding in York, UK. *Journal of Hydrology*, *546*, 419–436. https://doi.org/10.1016/j.jhydrol.2016.12.013

Committee on Earth Observation Satellites (CEOS). (2003). *The use of earth observing satellites for hazard support: Assessments & scenarios: Final report of the CEOS disaster management support group*. Universidad de Michigan.

Confederación Hidrográfica del Júcar (CHJ). (2011). *Elaboración de mapas de peligrosidad. Asistencia técnica para el desarrollo del sistema nacional de cartografía de zonas inundables en la Demarcación Hidrográfica del Júcar*. Author.

El Tiempo. (2008, May 18). Reportan un menor desaparecido tras fuerte aguacero en Barranquilla.

Enríquez de Salamanca, A. (2020). Victims crossings overflowing watercourses with vehicles in Spain. *Journal of Flood Risk Management*, *13*, e12645. https://doi.org/10.1111/jfr3.12645

Fitzgerald, G., Du, W., Jamal, A., Clark, M., & Hou, X. (2010). Flood fatalities in contemporary Australia (1997–2008). *Emergency Medicine Australasia*, *22*, 180–186. https://doi.org/10.1111/j.1742-6723.2010.01284.x

Francés, F., García-Bartual, R., Ortiz, E., Salazar-Galán, S., Blöschl, G., Komma, J., Habereder, C., Bronstert, A., & Blume, T. (2008). *Efficiency of non-structural flood mitigation measures: "Room for the river" and "retaining water in the landscape"* (CRUE Research Report No. I-6). General Directorate for Research in the European Commission.

Green, D., Yu, D., Pattison, I., Wilby, R. L., Bosher, L., Patel, R., Thompson, P., Trowell, K., Draycon, J., Halse, M., Yang, L., & Ryley, T. (2017). City-scale accessibility of emergency responders operating during flood events. *Natural Hazards and Earth System Sciences*, *17*, 1–16. https://doi.org/10.5194/nhess-17-1-2017

Hashimoto, T., Stedinger, J., & Loucks, D. (1982). Reliability, resiliency, and vulnerability criteria for water resource system performance evaluation. *Water Resources Research*, *18*, 14–20.

Johnson, S., & Yu, D. (2020). From flooding to finance: NHS ambulance-assisted evacuations of care home residents in Norfolk and Suffolk. *Journal of Flood Risk Management*, *13*(1), e12592. https://doi.org/10.1111/jfr3.12592

Jonkman, N., & Kelman, I. (2005). An analysis of the causes and circumstances of flood disaster deaths. *Disasters*, *29*(1), 75–97.

Kalantari, Z., Nickman, A., Lyon, S., Olofsson, B., & Folkeson, L. (2014). A method for mapping flood hazard along roads. *Environmental Management*, *133*, 69–77. https://doi.org/10.1016/j.jenvman.2013.11.032.x

Maples, L., & Tiefenbacher, J. (2009). Landscape, development, technology and drivers: The geography of drownings associated with automobiles in Texas floods, 1950–2004. *Applied Geography*, *29*, 224–234.

Martínez-Gomariz, E., Gómez, M., Russo, B., & Djordjević, S. (2017). A new experiments-based methodology to define the stability threshold for any vehicle exposed to flooding. *Urban Water Journal*, *14*(9), 930–939. https://doi.org/10.1080/1573062X.2017.1301501

Michielsen, A., Kalantari, Z., Lyon, S. W., & Liljegren, E. (2016). Predicting and communicating flood risk of transport infrastructure based on watershed characteristics. *Environmental Management*, *182*, 505–518. https://doi.org/10.1016/j.jenvman.2016.07.051

Milanesi, L., & Pilotti, M. (2019). A conceptual model of vehicles stability in flood flows. *Journal of Hydraulic Research*, *58*, 701–708. https://doi.org/10.1080/00221686.2019.1647887

Oshikawa, H., & Komatsu, T. (2014). Study on the risk evaluation for a vehicular traffic in a flood situation. *Proceedings of the 19th IAHR-APD Congress*, Hanoi, Vietnam.

Pregnolato, M., Ford, A., Wilkinson, S. M., & Dawson, R. J. (2017). The impact of flooding on road transport: A depth—Disruption function. *Transportation Research Part D*, *55*, 67–81. https://doi.org/10.1016/j.trd.2017.06.020

Salazar, S., Francés, F., Komma, J., Blume, T., Francke, T., Bronstert, A., & Bloschl, G. (2012). A comparative analysis of the effectiveness of flood management measures based on the concept of "retaining water in the landscape" in different European hydro-climatic regions. *Natural Hazards and Earth System Sciences*, *12*, 3287–3306. https://doi.org/10.5194/nhess-12-3287-2012

Samuels, P., Gouldby, B., Klijn, F., Messner, F., Sayers, P., Schanze, J., & Udale-Clarke, H. (2009). *Language of risk—Project definitions (2nd ed.)* (Report No. T32-04-01). Floodsite Consortium. Retrieved from http://www.floodsite.net/html/partner_area/project_docs/T32_04_01_FLOODsite_Language_of_Risk_D32_2_v5_2_P1.pdf

Shand, T., Cox, R., Blacka, M., & Smith, G. (2011). *Australian rainfall and runoff (AR&R). Appropriate safety criteria for vehicles. Australian rainfall and runoff, revision project 10* (Report No. P10/S2/020). Engineers Australia.

Shu, C., Xia, J., Falconer, R. A., & Lin, B. (2011). Incipient velocity for partially submerged vehicles in floodwaters. *Journal of Hydraulic Research*, *49*(6), 709–717. https://doi.org/10.1080/00221686.2011.616318

Smith, G. P., Modra, B. D., & Felder, S. (2019). Full-scale testing of stability curves for vehicles in flood waters. *Journal of Flood Risk Management*, *12*(2), e12527. https://doi.org/10.1111/jfr3.12527

Smith, G. P., Modra, B. D., Tucker, T. A., & Cox, R. J. (2017). *Vehicle stability testing for flood flows* (WRL Technical Report 2017/07). University of New South Wales.

Suárez, P., Anderson, W., Mahal, V., & Lakshmanan, T. (2005). Impacts of flooding and climate change on urban transportation: A system wide performance assessment of the Boston Metro Area. *Transportation Research Part D*, *10*, 231–244. https://doi.org/10.1016/j.trd.2005.04.07

Teo, Y., Falconer, R., Lin, B., & Xia, J. (2012). Investigations of hazard risks relating to vehicles moving in flood. *Water Resources Management*, *1*, 52–66.

Toda, K., Ishigaki, T., & Ozaki, T. (2013). Experiment study on floating car in flooding. In *International conference on flood resilience experiences in Asia and Europe, 5–7 September 2013, Exeter, UK*. ICFR.

UNISDR. (2009). *Terminología sobre reducción del riesgo de desastres. Estrategia para la reducción de desastres de las Naciones Unidas*. Retrieved from https://floodresilience.net/resources/item/terminologia-sobre-reduccion-del-riesgo-de-desastres

Versini, P. A., Gaume, E., & Andrieu, H. (2010). Assessment of the susceptibility of roads to flooding based on geographical information–test in a flash flood prone area (the Gard region, France). *Natural Hazards and Earth System Sciences*, *10*, 793–803.

Xia, J., Falconer, R. A., Xiao, X., & Wang, Y. (2014). Criterion of vehicle stability in floodwaters based on theoretical and experimental studies. *Natural Hazards*, *70*(2), 1619–1630. https://doi.org/10.1007/s11069-013-0889-2

Xia, J., Teo, F., Lin, B., & Falconer, R. (2011). Formula of incipient velocity for flooded vehicles. *Natural Hazards*, *58*(1), 1–14. https://doi.org/10.1007/s11069-010-9639-x

Yin, J., Yu, D., Yin, Z., Liu, M., & He, Q. (2016). Evaluating the impact and risk of pluvial flash flood on intra-urban road network: A case study in the city center of Shanghai, China. *Journal of Hydrology*, *537*, 138–145. https://doi.org/10.1016/j.jhydrol.2016.03.037

How to cite this article: Bocanegra, R. A., & Francés, F. (2021). Assessing the risk of vehicle instability due to flooding. *Journal of Flood Risk Management*, e12738. https://doi.org/10.1111/jfr3.12738